16th World Conference on Earthquake, 16WCEE 2017
Santiago Chile, January 9th to 13th 2017
Paper N° 2729
Registration Code: S-F1462953149

APPLICATION OF A NEW METHODOLOGY FOR SEISMIC TORSION DESIGN TO A MULTI-STORY BUILDING STRUCTURE

K.R. Hwang[(1)], H.S. Lee[(2)], A.R. Ali[(3)]

[(1)] Research Professor, School of Civil, Environmental, and Architectural Engineering, Korea University, dh8149@korea.ac.kr
[(2)] Professor, School of Civil, Environmental, and Architectural Engineering, Korea University, hslee@korea.ac.kr
[(3)] Graduate student, School of Civil, Environmental, and Architectural Engineering, Korea University, ruthali@korea.ac.kr

Abstract

An experimental research using a 1:5 scale five-story reinforced concrete building model with the irregularities of a soft/weak story and torsion at the ground story revealed that the design eccentricity used in the general codes in itself cannot represent the critical torsional behaviors not only because the range of eccentricities at the peak responses in the time histories of drift and base shear exceeded the range of eccentricity predicted by the code, but also because under severe ground excitations even very small eccentricity does not necessary translate into a small but significantly large drift at the edge frame. To overcome this problem, instead of using the eccentricity as design parameter, a completely new methodology in the design or control of torsionally unbalanced building structures is proposed by defining the design torsional moment in a direct relationship with the shear force given as an ellipse with the maximum points in its principal axes located by the two adjacent torsion-dominant modal spectral values. In this paper, the proposed methodology is applied to the design of a torsionally unbalanced five-story RC building model. Linear and nonlinear time history analyses of the building model are carried out, and the torsional behaviors of the structure designed according to the proposed methodology are evaluated by comparing demand and supply in shear versus torsion relationships in each story.

Keywords: torsion; irregularity; time history analysis

1. Introduction

The severe damage and collapse of building structures in earthquake can occur through several phenomena, one of which is the torsion due to the eccentricity between the inertia force and resisting force. To prevent excessive deformation, damage, and collapse caused by torsion, the current seismic design code specifies two torsion design approaches: First, is the use of equivalent lateral force (static) procedure, where the structure is designed by the most adverse combination of the seismic forces and the design eccentricities given in Eqs. (1) and (2) as shown in Fig. 1(a). Second, is the use of the dynamic analysis such as modal response spectrum analysis or time history analysis, where the center of the mass (CM) at each story is assumed to be the positions, CM1~CM4 in Fig. 1(b). The most adverse results in deformations and member forces of the structure obtained from the dynamic analysis are used for design.

$$V_D = C_S W \tag{1}$$

$$e_d = \alpha e_s + \beta b \quad \text{or} \quad e_d = \delta e_s - \beta b \tag{2}$$

where, V_D is the seismic base shear; C_S is the seismic coefficient; W is the effective seismic weight; e_d is the design eccentricity composed of static and accidental eccentricities; e_s is the static eccentricity determined as the distance between the CM and CS (center of stiffness); βb ($=e_a$) is the accidental eccentricity, which is included to consider torsional effects due to the uncertainty of CM and CS, the rotational component of ground motion, and other uncertainties not explicitly considered; b is the plan dimension of the building perpendicular to the direction of ground motion; and α, β, and δ are code-specified coefficients.

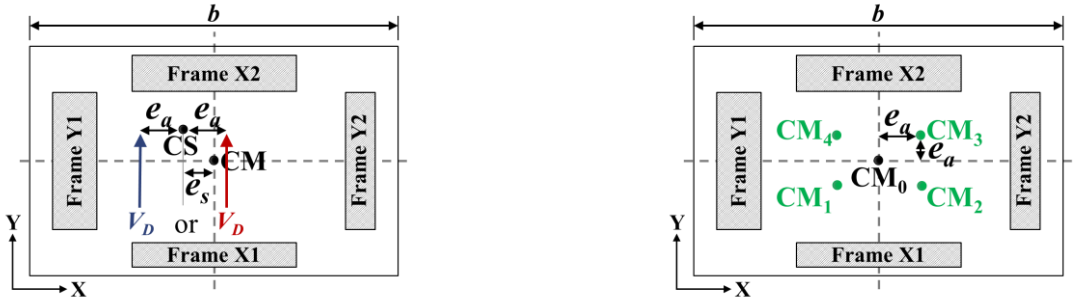

(a) Equivalent lateral force (static)analysis (b) Dynamic analysis

Fig. 1 Conventional torsion design approaches

Though the design eccentricity in Eq. (2) is based on the linear elastic behavior of the structure, the main concern is the control of the deformation and damage in the inelastic range. That is, the objective of torsion design is that the maximum drift or ductility demands in any part of the element of the torsionally unbalanced building do not exceed those of the torsionally balanced, under any circumstances. However, almost all researchers aimed at the reasonable determination of coefficient values, α, β, and δ in Eq. (2), to achieve such an objective, based on the assumption that the satisfaction of design requirements for load combinations of the seismic design story or base shear forces, V_D, and the torsional moment resulting from the design eccentricity ensures the desirable inelastic behavior under the severe earthquake. Although it is difficult to find a sound rationale that the satisfaction of design requirements for four load combinations determined by Eq. (2) guarantees the desirable inelastic behavior, researchers and engineers have maintained the faith in efficacy of the design eccentricity for over six decades since the emergence of earthquake engineering as a new field of engineering [1].

In this study, to overcome the serious limitations of the conventional torsion design approach using the design eccentricity, a new simple, transparent, and comprehensive torsion design approach is proposed based on actual torsional behaviors obtained through the shake-table test of a low-rise RC building model, which has a high degree of irregularity of soft story, weak story, and torsion at the ground story [2~4]. In addition, the proposed methodology is applied to the design of a torsionally unbalanced five-story RC building model. Linear and nonlinear time history analyses of the building model have been carried out, and the torsional behaviors of the structure designed according to the proposed methodology are evaluated by comparing demand and supply in shear versus torsion relationships in each story.

2. Experimental research using a 1:5 scale five-story reinforced concrete building

2.1 Design of the model and experimental setup

The prototype in Fig. 2 was determined based on the inventory study, and designed by considering the gravity loads only. The reinforcement details are non-seismic, according to construction practice in Korea. The lowest two stories of the 1:5 scale structure model were designed and constructed to strictly satisfy the similitude requirements, while the upper three stories were replaced with concrete blocks of similar volume. This modified model enabled a reduction in time and cost for construction, without significant loss of similitude in the response. To complement the irregularity of the original model (i.e., soft story, weak story, and torsional eccentricity at the ground story) the prototype was strengthened with buckling-restrained braces (BRB's) and fiber reinforced polymer (FRP) sheets in the peripheral frames. Detailed designs of the BRB's and FRP sheets are provided in Lee et al. [3]. Evaluations of the prototypes regarding the irregularities, in accordance with KBC 2005 [5], are provided in Table 1. The degrees of irregularity of the original building were so high at the ground story that even the strengthened building still did not satisfy the requirement for regularity in some cases. The stiffness and strength of the strengthened first story were increased slightly, compared with those of the second story, because the ratio of the wall area to the total floor area at the second story, 10.5%, is much larger than that at the first story 1.93%. However, the strengthened model greatly alleviated the degree of irregularity for the torsion in the Y- direction (Table 1).

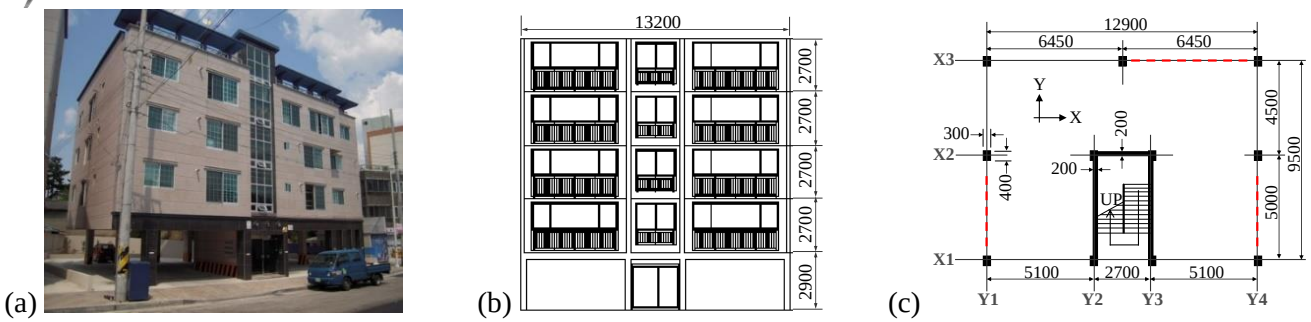

Fig. 2 Prototype structure (unit: mm): (a) Example of piloti building; (b) Elevation; and (c) Plan of the ground floor

Table 1. Assessment of irregularity at the ground story according to KBC2005 [5]

Irregularity	Criteria	Original		Strengthened	
		X-dir.	Y-dir.	X-dir.	Y-dir.
Stiffness	If $K_1/K_2 < 0.7$, irregular (NG)	0.159 (NG)	0.160 (NG)	0.218 (NG)	0.213 (NG)
Strength	If $F_1/F_2 < 0.8$, irregular (NG)	0.181 (NG)	0.284 (NG)	0.260 (NG)	0.356 (NG)
Torsion	If $\delta_{max}/\delta_{avg} > 1.2$, irregular (NG)	1.18 (OK)	1.82 (NG)	1.26 (NG)	1.31 (NG)

K_1/K_2: Stiffness of first story / stiffness of second story, F_1/F_2 : Strength of first story / strength of second story, $\delta_{max}/\delta_{avg}$: Maximum / average drift

The design base shear force, V, was determined using the following Eqs (3) and (4) with the response modification factor, R = 3, and the occupancy importance factor, I_E =1.2, as defined in KBC 2005 [5]:

$$V = C_s \cdot W = 0.176 \cdot 7{,}148 = 1{,}260\ kN \text{ (prototype)} \tag{3}$$

$$C_S = \frac{S_{D1}}{(R/I_E)T_a} = \frac{0.234}{(3.0/1.2)\,0.349} = 0.268, \text{ but, not exceeding, } C_S = \frac{S_{DS}}{R/I_E} = \frac{0.439}{3.0/1.2} = 0.176 \tag{4}$$

where C_s is the seismic coefficient; W is the seismic weight of the prototype building; S_{DS} and S_{D1} are the spectral accelerations at period 0.2 s and 1 s, respectively; and T_a is the fundamental period.

The experimental set-up and instrumentation to measure the displacements, accelerations, and forces for the second series of tests are similar to those of the first series of tests, and are shown in Fig. 3. The target or input accelerogram of the table was based on the recorded 1952 Taft N21E (X direction) and Taft S69E (Y direction) components, and was formulated by compressing the time axis with a scale factor of $1/\sqrt{5}$, and by adjusting the peak ground acceleration (PGA), to match the corresponding elastic design spectrum in KBC 2005 [5]. The strengthened model was tested not only up to the levels of the maximum considered earthquake (MCE) in Korea, but also to the level of the design earthquake in San Francisco, USA. Detailed information on the results of earthquake simulation tests on the original and strengthened model is provided in Lee et al [2~3]. The program of earthquake simulation tests on the strengthened model is summarized in Table 2.

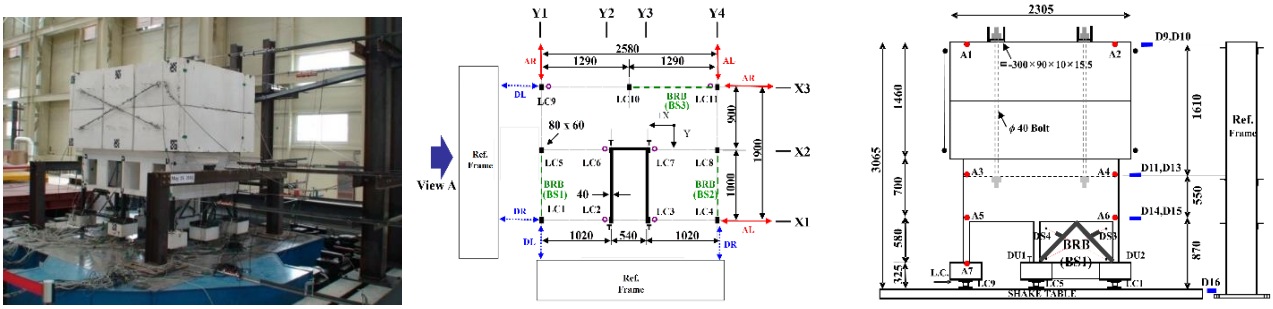

(a) Overview of earthquake simulation test set-up

(b) Plan at the ground story

(c) View A (D: displacement, A: acceleration)

Fig. 3 Dimensions and instrumentation of the 1:5 scale structure model (unit: mm)

Table 2. Test program (X-Taft N21E, Y-Taft S69E)

Test designation	Intended PGA(g)		Measured PGA(g)		Return period in Korea (year)
	X-dir.	Y-dir.	X-dir.	Y-dir.	
R0.070X	0.07	-	0.083	-	50
R0.070XY	0.07	0.08	0.072	0.097	(Service Level EQ. SLE)
R0.187X	0.187	-	0.174	-	Design Earthquake (DE)
R0.187XY	0.187	0.215	0.147	0.220	
R0.3X	0.3	-	0.261	-	2400 (MCE)
R0.3XY	0.3	0.345	0.250	0.374	
R0.4X	0.4	-	0.329	-	DE in San Francisco, USA
R0.4XY	0.4	0.46	0.442	0.509	

2.2 Seismic interaction between shear and torsion

The design eccentricity is composed of static and accidental eccentricity (Eq. (2)). In this experimental model, however, the center of mass in the plan was unchanged throughout the tests, and the shake table did not rotate during the earthquake simulation. Thus, in this study, we investigated how the center of resistance (CR) changed in the elastic and inelastic response under uni- and bi-directional excitations, with increasing intensity of the excitations.

In Fig. 4, instants (1) to (4) represent the maximum responses of the interstory drift at frames X1 and X3, and instants (5) and (6) indicate the maximum responses of the torsional deformations. Instants of the maximum torsional deformation (instants (5) and (6)) always had lower drifts, than those at instants (1) to (4), at frames X1 and X3. In the elastic range under R0.070XY, the eccentricities, $e_y=T_x/V_x$, at instants (1) to (4) occurred within a range of ±35% from the CM, while those in the inelastic range under R0.3XY occurred within a range of ±15% from the CM. The eccentricities at instants (5) and (6) were considerably larger than those at instants (1) to (4). The model had larger eccentricities during the elastic response, R0.070XY, than those during inelastic response, R0.3XY (Fig. 4). Again, the higher intensity of excitations caused the lower values of eccentricity. The reason for this reduction is considered to be the significantly increased contribution of the transverse frames to the total torsional resistance.

The ratio of the torsional moment contributed by the Y-directional frames to the total, T_y/T_{total}, for all tests is shown in Fig. 4. Most of the T_y/T_{total} ratios were larger than 50%. For example, the T_y/T_{total} ratio at instant (2) representing the maximum translational drift at frame X1 under R0.3X was 100%, while the T_y/T_{total} ratio at instant (1) at frame X1 was 60%. Generally, the higher the intensity of excitations, the larger T_y/T_{total} ratios the model had.

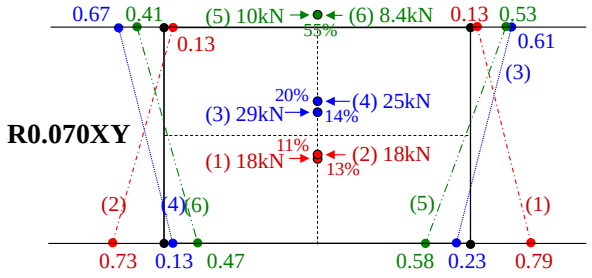

R0.070XY	(1)	(2)	(3)	(4)	(5)	(6)
T_y (kNm)	5.39	6.97	8.20	14.04	13.78	13.48
T_x (kNm)	4.52	3.89	8.38	9.90	10.71	9.41
T_y/T_{total}	54%	64%	49%	59%	56%	59%

(a)

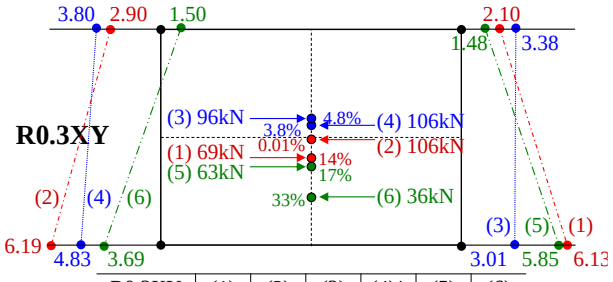

R0.3XY	(1)	(2)	(3)	(4)*	(5)	(6)
T_y (kNm)	28.83	27.94	7.54	9.33	32.75	36.58
T_x (kNm)	19.39	-0.02	9.00	-7.89	20.61	23.82
T_y/T_{total}	60%	100%	46%	N.A.	61%	61%

* Instant (4), $T_{total} = T_x + T_y = -7.89 + 9.33 = 1.44 kNm \approx 0$

(b)

Fig. 4. Distributions of interstory drifts and locations of CR at instants (1) to (6): (a) SLE; and (b) MCE in Korea

The seismic interaction between shear and torsion under the serviceability level of the earthquake (SLE, R0.070XY) and the maximum considered earthquake (MCE, R0.3XY) in Korea is presented in Fig. 5. The response histories of the X-directional base shear versus torsional moment contributed by the X-directional frames V_x-T_x in the elastic range under R0.070XY (Fig. 5(a)) and inelastic range under R0.3XY (Fig. 5(b)) appear very chaotic. The eccentricity in the X direction, $e_y=T_x/V_x$, appears to be not in a limited range as prescribed in the general codes, but it varied from zero to infinity with the variation of the torsional moment and the base shears for both elastic and inelastic responses. Under MCE in Korea (R0.3XY), the inertial torque varied from –23.1kNm to +27.9kNm and the eccentricity varied from 3.7% to 0.01% with the yielding base shear, 106kN, being almost constant for a short duration from 3.04s to 3.11s (a→(4)→(2)). The small eccentricity of 0.01% at time instant (2) did not necessarily translate into a small but significantly large rotation (0.00173rad) leading to the maximum drift (6.2mm) at the edge frame in Fig. 7(a) due to a high level of inertial torque (27.9kNm) and a significantly degraded torsional stiffness caused by yielding of the longitudinal frames. Based on these observations, it becomes clear that the eccentricity in itself cannot represent the real critical torsional behavior as design parameter.

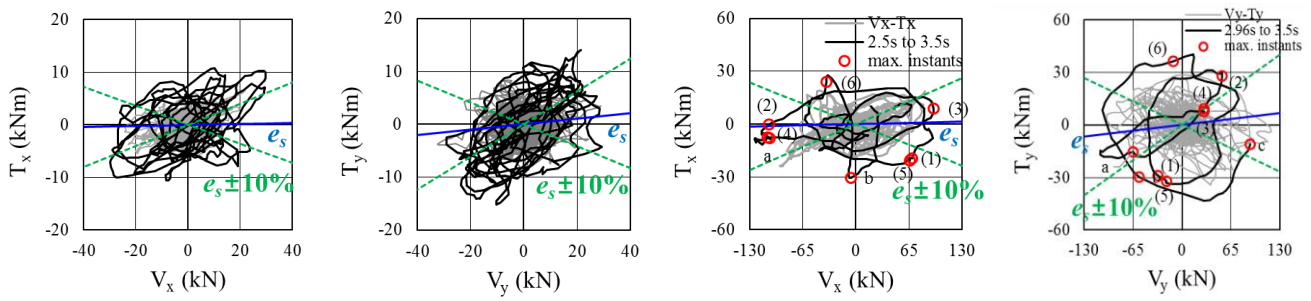

(a) R0.07XY (SLE) (b) R0.3XY (MCE)

Fig. 5 Seismic interaction between shear and torsion

Using the yield strength of each frame in the simplified bilinear force-displacement relation, the yield shear force and yield torsional moment with the yield mechanism are shown by closed envelope line in Fig. 6. It is called the base shear-torque (BST) corresponding yield surface [6]. The response histories of base shear (V) versus torsional moment (T_{total} & T_y) under MCE in Korea under R0.3XY are also presented in Fig. 6. The demand (T_{total}) and supply (capacity) for the shear force and the torsional moment are directly compared. Each segment of straight lines in Fig. 7 corresponds to the state of yielding mechanism as depicted beside the lines. In Fig. 6(a), the large X-directional base shears at time instant (2) exceeded the plane EF of the BST surface. In Fig. 6(b), the point "b" in the curves of the Y-directional base shear versus the torsional moment can be found to be near the BST yielding surface. The corresponding states of forces and deformation are given in Fig. 7.

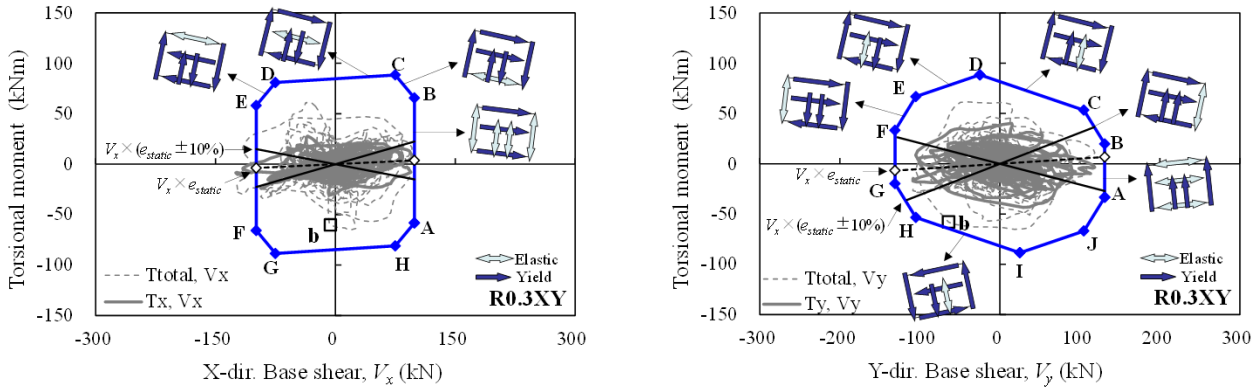

(a) V_x-T (b) V_y-T

Fig. 6 BST yield surface versus V-T response histories under R0.3XY [4]

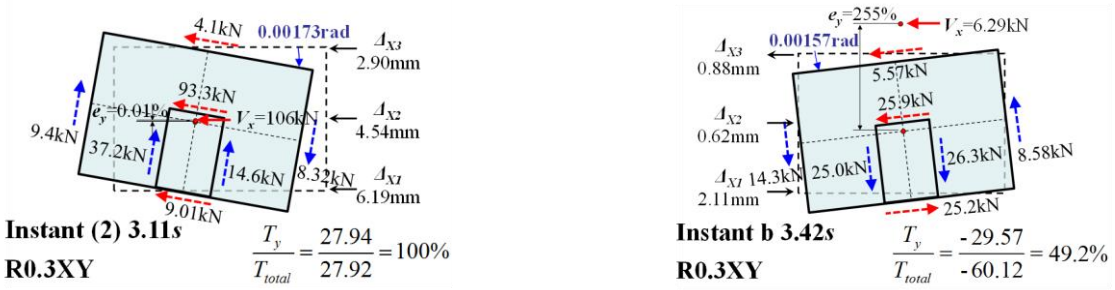

(a) Instant (2) (b) Instant b

Fig. 7 Distribution of frame forces and deformation at time instants (2) and b in Fig. 6(b) [4]

3. A new methodology in seismic torsion design

The actual dynamic coupling existing between lateral and torsional motions in a building with plan asymmetry, named "natural torsion" [7], inevitably leads to non-uniform displacement demands on the lateral resisting planes of the system. Such displacement demands are of key interest in the sizing and detailing of structural elements for earthquake resistance. The relation of torsional moment and base shear, T_x-V_x and T_y-V_y, in the experiment is presented in Fig. 6. The eccentricity, which is the slope of the line connecting the zero point and the point (T_x, V_x) varies from zero to infinity at each instant. The experimental relationship contains both natural and accidental torsions. In this experimental model, the accidental torsion includes only the uncertainty on the stiffness of the structures, because the center of mass in the plan was unchanged and the shake table did not rotate throughout the tests. The natural torsion for the experimental model was simulated through the elastic modal time history analysis using SAP2000 [8], using the record of the table acceleration under R0.07X, which is assumed to be the serviceability level for an earthquake in Korea. For the five natural modes of the model which constitute the time history, the natural periods and modal participating mass ratios are given in Table 3, where the first and second modes are the modes coupled by the translational movement in the X direction and the torsion, while the third is translation in the Y direction. The fourth and fifth are the second translational modes in the X- and Y- directions, respectively. While the participating mass ratio of the X-directional translation, M_{ux}, is 58% with that of the torsion, M_{rz}, being 30% for the first mode, the participating mass ratio of torsion, M_{rz} = 68%, is dominant over that of the X directional translation, 25%, for the second mode.

Table 3. Periods and modal participating mass ratios (M) obtained from elastic modal analysis

	Mode 1	Mode 2	Mode 3	Mode 4	Mode 5
Periods (Experiment)*	0.175 sec	0.160 sec	0.142 sec	-	-
Periods (Modal analysis)	0.166 sec	0.157 sec	0.145 sec	0.0546 sec	0.0428 sec
M_{ux}**	58.0 %	25.0 %	0.0 %	17.0 %	0.0 %
M_{uy}**	0.0 %	2.0 %	70.0 %	0.0 %	28.0 %
M_{rz}**	30.0 %	68.0 %	2.0 %	0.0 %	0.0 %

* Periods are obtained from the earthquake simulation test results (time histories of base shear and torsional moment) under R0.07X using Fast Fourier Transforms (FFT) analysis.

** M_{ux} and M_{uy}: the X- and Y directional modal participating mass ratios, respectively. M_{rz}: the torsional modal participating mass ratio.

In Fig. 8, the total analytical relationship generally simulated well the experimental, and that the modal responses in the relationship between the torsional moment and base shear for the (i) first and (ii) second modes, (iii) the combination of the first and the second, and (iv) the comparison of the experimental responses with the total analysis, comprising all the responses of the five modes under R0.070X. In Fig. 8 the torsional moment-base shear responses, T_x-V_x, in modes 1 and 2 reveal the linear relationship. The slope in the T_x-V_x relationship of the first mode, $e_y = T_x/V_x$, is -7.8%, with that of the second mode, $e_y=T_x/V_x$, being 21.5%. The T_x-V_x relationship, combining the first and second modal behaviors, resulted in the elliptical shapes, where the maximum values in base shear and torsional moment in the first and second modes were generally preserved while the eccentricity was no longer constant, but varied from zero to infinity. This phenomenon is also investigated in the relationship

between the torsional deformation and the X-directional interstory drift at the first story, θ - Δ_x, in Fig. 8 (c). The response histories of θ - Δ_x in modes 1 and 2 reveals the linear relationship, and the boundary of the response histories combining the first and second modal behaviors looks like the ellipse.

These elliptical responses reveal the reason for the gap between the values of static eccentricity assumed in the seismic design codes, which generally represent the first translation and torsion coupled mode, and those of the 'real' dynamic eccentricity, that is, the natural eccentricity. It is also noteworthy that the combined modal behaviors, that is, mode 1 + mode 2, approximate roughly the total results of elastic modal analysis, which, in turn, simulate very well the experimental results.

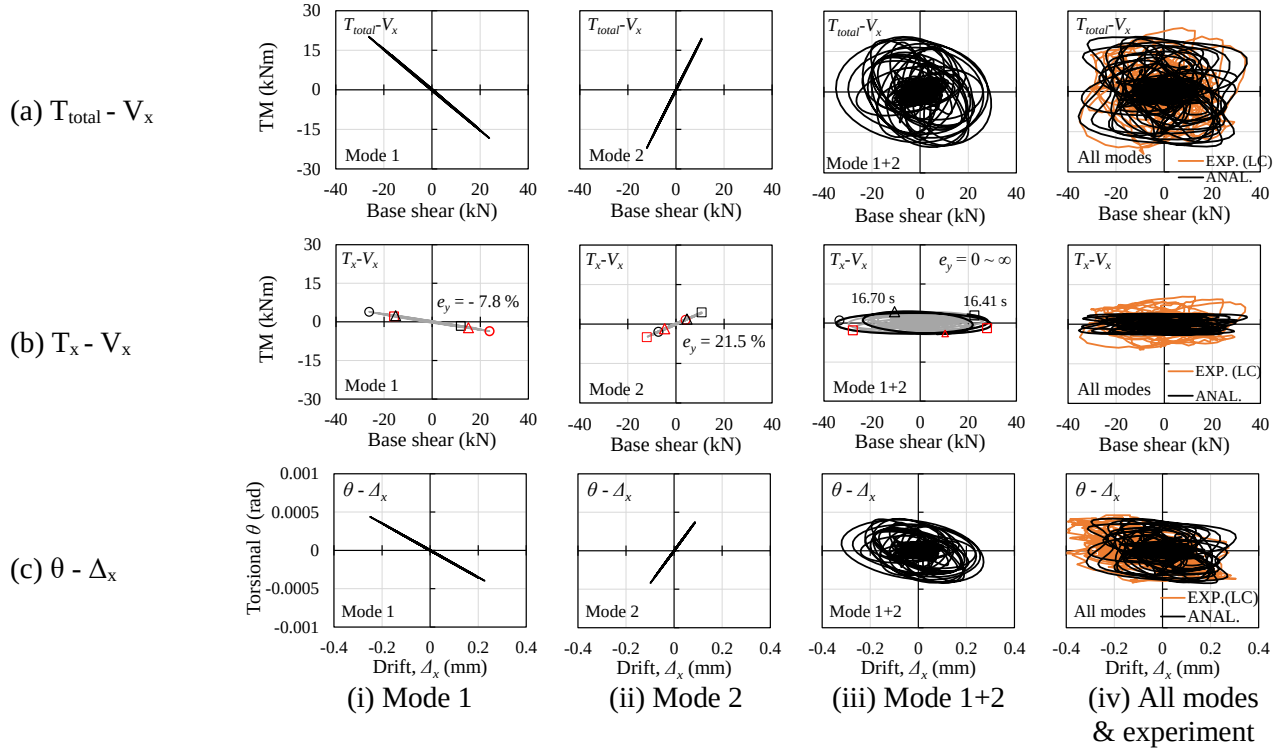

Fig. 8 Results of elastic modal analysis under R0.07X compared with corresponding experiment

An ellipse with the response histories of T_{total}-V_x and θ-Δ_x combining the first and second modal responses is presented in Fig. 9 with those of modal responses. The ellipse is constructed using the maximum values in the first and second modes in the T_{total}-V_x and θ-Δ_x relationships (Fig. 8). The equation of ellipse can be expressed as the path of a point ($X(t)$, $Y(t)$) in Eq. (5):

$$X(t) = A\cos t\cos\varphi - B\sin t\sin\varphi$$
$$Y(t) = A\cos t\sin\varphi + B\sin t\cos\varphi \quad (5)$$

where, t is the parametric angle, $0 \le \theta \le 2\pi$; A is radius in the major axis; B is the radius in the minor axis; and φ: the angle between the X-axis and the major axis of the ellipse. The parameters A, B, and φ in Eq. (5) are given in Table 4. We can find that the constructed ellipse covers reasonably the actual response histories as shown in Fig. 9.

Table 4. Parameters in equation of ellipse (Eq. (5)) for shear-torsion relationships

Relationship of Ellipse		$X(t)$: Shear		$Y(t)$: Torsion		A	B	ϕ
		1st mode	*2nd mode*	*1st mode*	*2nd mode*			
Serviceability level for EQ. in Korea (R0.07X) (Fig. 9)	Force*	$V_{x,max1}$	$V_{x,max2}$	$T_{total,max1}$	$T_{total,max2}$	1.41	1.19	-0.785
		26.3	12.1	20.1	22.1			
	Deformation*	$\Delta_{x,max1}$	$\Delta_{x,max2}$	θ_{max1}	θ_{max2}	1.41	1.03	-0.785
		0.25	0.098	0.000439	0.000419			

* Unit of force, V and T: kN and kNm, respectively; Unit of deformation, Δ and θ: mm and rad, respectively.

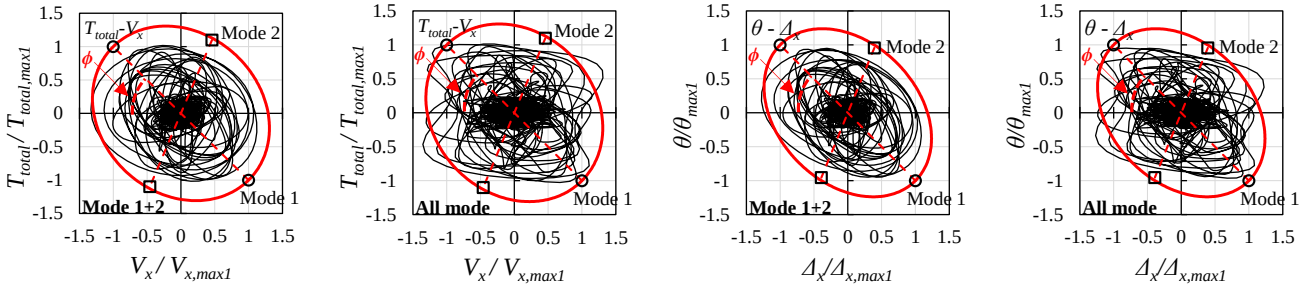

(a) Force relationship (b) Deformation relationship

Fig. 9 Shear-torsional force and deformation relationship under R0.07X

4. Application of the proposed methodology to a five-story RC building

4.1 Design of the structure

The proposed methodology is applied to a torsionally unbalanced five-story two-by-two bay RC building structure as shown in Fig. 10, which was designed according to KBC 2009 [5]. The irregularities of this structure are evaluated in accordance with KBC 2009. The degree of torsional irregularity of this structure is 1.27, which exceeds the limit value of 1.2. The properties of columns and beams are given in Fig. 10(a). A design concrete strength (f'_c) is 21MPa with the reinforcement yield strength of 400MPa. The dead load (DL) is 8,110kN. The effective seismic weight (W) is set as the DL.

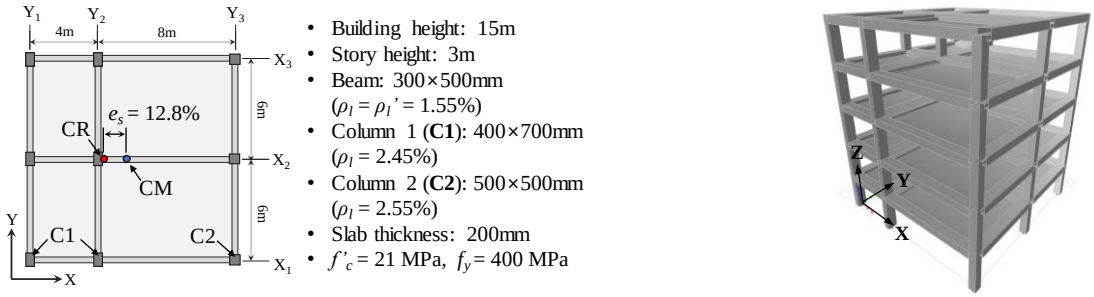

(a) Plan (b) Analytical model (ETABS)

Fig. 10. Torsionally unbalanced five-story two-by-two bay RC building structure

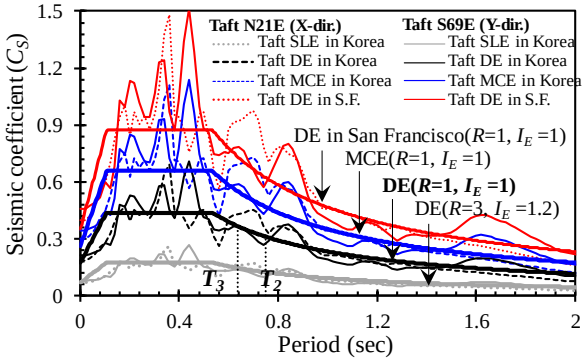

Fig. 11. Comparison with elastic design spectra and response spectra of input ground motions (1952 Taft EQ.)

4.2 Analytical model

Linear and nonlinear time history analyses of the building structure were carried out using ETABS [9]. An overview of the analytical model is given in Fig. 10(b). The elastic stiffnesses of components for axial, bending, and shear behaviors used initial values of EA_g, EI_g, and $0.4EA_g$, respectively. Beams are modeled as elastic beam elements with nonlinear moment-rotation (M-θ) hinges at the ends of the beam, which are specified in the recommendation of ASCE 41-13 [10]. Columns are modeled as inelastic column elements by using the inelastic

fiber section accounting for longitudinal reinforcement and confined/unconfined concrete, which can describe the inelastic axial and bending behaviors. We neglect the inelastic shear behaviors of beam and column. Damping ratios follow the Rayleigh damping with a damping of 3.0% at the first and fourth periods, T_1 and T_4, respectively. The seismic mass was lumped at the CM (Fig. 10(a)) of each floor regarding the gravity load and the associated rotational moment of inertia. After the gravity load analysis, a nonlinear time history analyses were conducted. The input ground motions are derived from the recorded Taft N21E (X-dir.) and S69E (Y-dir.) components by adjusting the PGA corresponding to the elastic response spectra to SLE in Korea, DE in Korea, MCE in Korea, and DE in San Francisco as shown in Fig. 11.

4.3 Application of proposed methodology

To obtain an elliptical design demand, firstly, an elastic modal analysis was conducted. The input ground motion corresponding to SLE in Korea is used in the Y direction only. For the six natural modes of the structure, the natural periods and the modal participating mass ratios are given in Table 5. The second and third modes are the modes coupled by the translational movement in the Y direction and torsion, while the first mode is translation in the X direction. In Fig. 12, the relationship between T_{total} and V_y in the second and third modes is obtained from the results of the modal time history analysis from which the static eccentricities of each mode, e_{x2} and e_{x3}, can be derived. An ellipse combining the second and third modal values in the relationship of T_{total}-V_y covers the response histories of all modes reasonably well.

Table 5. Periods and modal participating mass ratios (M) of five-story two-by-two bay frame structure

	Mode 1	**Mode 2**	**Mode 3**	Mode 4	Mode 5	Mode 6
Periods (sec)	0.802s	**0.750s**	**0.637s**	0.259s	0.239s	0.197s
M_{ux}^*	81.9%	**0%**	**0%**	11.7%	0%	0%
M_{uy}^*	0%	**38.2%**	**41.7%**	0%	4.92%	7.32%
M_{rz}^*	0%	**43.3%**	**38.1%**	0%	6.7%	4.98%

* M_{ux} and M_{uy}: the X- and Y directional modal participating mass ratios, respectively. M_{rz}: the torsional modal participating mass ratio.

Based on the proposed methodology, the design demand is defined as an ellipse with two adjacent torsion-dominant modal spectral values using the design spectrum (C_{s2} and C_{s3}, Fig. 11) and the results of modal analysis, which are the periods (T_2 and T_3), the modal participating mass ratios (M_{uy2} and M_{uy3}) and the static eccentricities (e_{x2} and e_{x3}):

$$\text{Design base shear: } V_{D2} = C_{s2}M_{uy2}W = 421\text{kN; and } V_{D3} = C_{s3}M_{uy3}W = 541\text{kN} \quad (6)$$

$$\text{Design torsional moment: } T_{D2} = (e_{x2}b)V_{D2} = 2{,}700\text{kNm; and } T_{D3} = (e_{x3}b)V_{D3} = -2{,}350\text{kNm} \quad (7)$$

The ellipse is constructed using the values of V_{D2}-T_{D2} and V_{D3}-T_{D3} as shown in Fig. 13. Comparing the ellipse with the SST yield surface which is obtained from the yield strength of each frame in the simplified bilinear force-displacement relation with the yield mechanism (Fig. 14(a)), the elliptical demand is within the SST yield surface (capacity). This approach provides a simple and transparent conceptual design tool through comparison with the torsion capacity diagram given as SST yield surfaces without having to perform dynamic time history analyses.

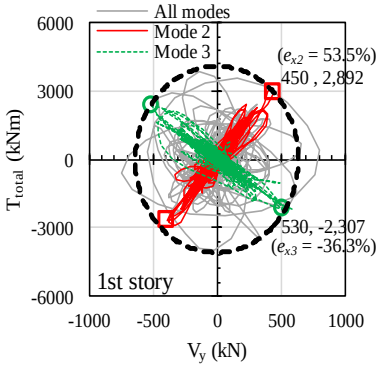

Fig. 12. Shear force-torsional moment relationship obtained from elastic modal analysis

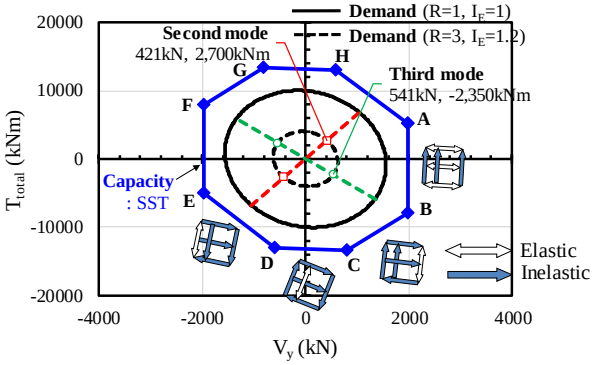

Fig. 13. Design diagram using shear force-torque relationship

4.4 Seismic interaction between shear and torsion

To evaluate the efficacy of the proposed methodology, we investigated the linear and nonlinear behaviors of the structure in the format of story shear versus story torsion throughout nonlinear time history analysis in the two orthogonal (X and Y) directions simultaneously with the increase of the level of earthquake intensity such as SLE, DE, and MCE in Korea and DE in San Francisco. The hysteretic relationships between the base shear and the first-story drift in the X and Y directions are shown in Fig. 14(b). Under SLE in Korea, elastic behavior is observed. A small amount of energy dissipation occurred under DE and MCE in Korea, and larger inelastic behaviors are observed under DE in San Francisco.

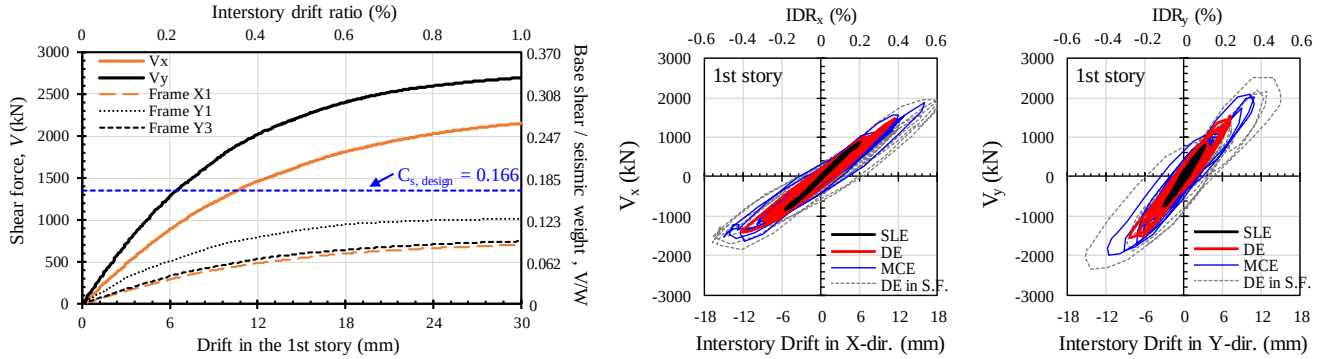

(a) Capacity curves (b) Results of time history analysis

Fig. 14. Relationship between base shear and first story drift in the X and Y directions

In Figs. 15 and 16, time instants (1) and (2) denote the maximum responses of the interstory drift at a frame Y3 (Fig. 10(a)), and instants (3) and (4) indicate the maximum responses of the torsional deformations. Fig. 15 illustrates the seismic interaction between shear and torsion in the first story under SLE in Korea and DE in San Francisco. The response histories of the Y-directional base shear versus torsional moment contributed by the Y-directional frames V_y-T_y in the elastic range under SLE (Fig. 15(a)-2) and the inelastic range under MCE (Fig. 15(b)-2) appear very chaotic. The eccentricities, $e_x=T_y/V_y$ and $e_y=T_x/V_y$, vary from zero to infinity with a variation of the torsional moment and the base shears for both elastic and inelastic responses. The e_x at time instant (3) is -105% b and -95% b under SLE in Korea and DE in San Francisco, respectively, which is significantly larger than the value of eccentricity predicted by the code, $e_s \pm 5\% = -12.8\% \pm 5\%$.

Despite the chaotic responses in V-T (Figs. 15(a)-2, (a)-3, (b)-2, and (b)-3) and V_x-V_y (Figs. 15(a)-4 and (b)-4), a linear trend is observed in the relationship of T_x-T_y in the elastic range under SLE in Korea (Fig. 15(a)-1) with the ratio of T_x:T_y = 40%:60%, except at time instants of the peak translational behaviors in the Y direction. At time instant (1) after reaching the maximum base shear in the Y direction, most of the inertial torque is resisted by the perpendicular (X-dir.) frames (T_x=705kNm and T_y=220kNm). This phenomenon is also observed in the inelastic range under DE in San Francisco (Fig. 15(a)-2). In addition, a torsional stiffness in the inelastic range is significantly degraded to 54% of initial stiffness as shown in Fig. 15(b)-5.

In Figs. 16 (a) and (b), the relations between the torsional moment and story shear force (T_{total}-V_y and T_y-V_y) under DE in San Francisco are compared with the SST yield surface in the first and second stories, respectively, with the distribution of interstory drifts and locations of CR at instants (1) to (4). The seismic responses in the first and second stories exceed lines AB and EF of SST yield surface, which indicate that the frames parallel to the excitation have yielded in the positive and negative directions. This can be observed from the distribution of interstory drifts. At instants (1) and (2), the interstory drifts in the Frames Y1, Y2, and Y3 exceed the yield drift of each frame in Fig. 14(a). Figs. 16 (a) and (b) also include the ratio of the torsional moment contributed by the Y-directional frames to T_{total}. Instant (1) in the first and second stories with a small value of the total torque reveal the counteracting T_x and T_y after yielding of all Y-directional frames, and 35% and 49% of the inertial torques are resisted by the Y-directional frames at instant (2) in the first and second stories, respectively. At instants of the maximum torsional deformation in the first story, (3) and (4), however, the ratios of T_y/T_{total} are 63.6% and 59.0%, respectively, which are similar to those under SLE in Korea in Fig. 15(a)-1, despite of presence of torsional stiffness degradation.

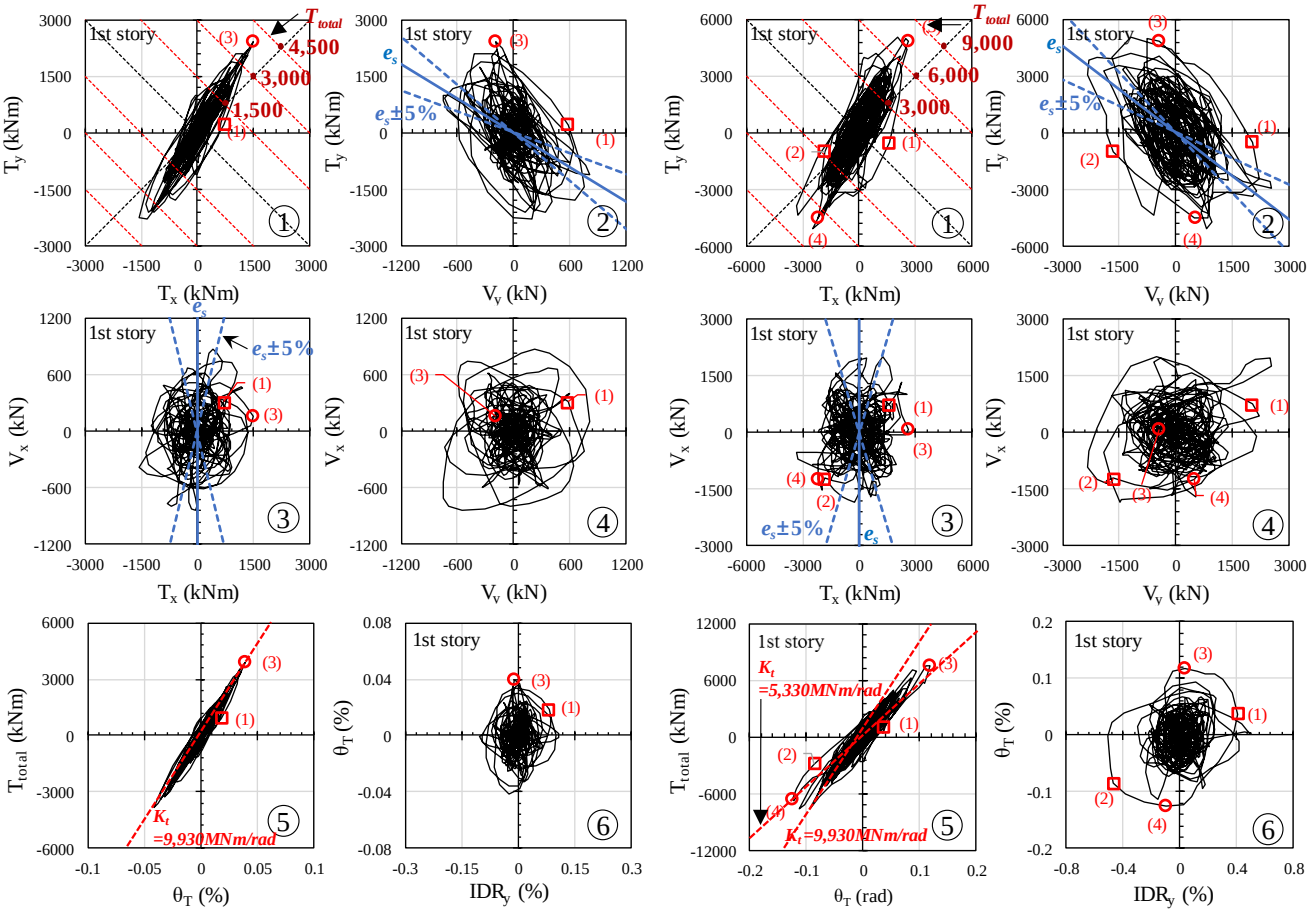

(a) SLE (b) DE in San Francisco

Fig. 15 Seismic interaction between shear and torsion under SLE in Korea and DE in San Francisco

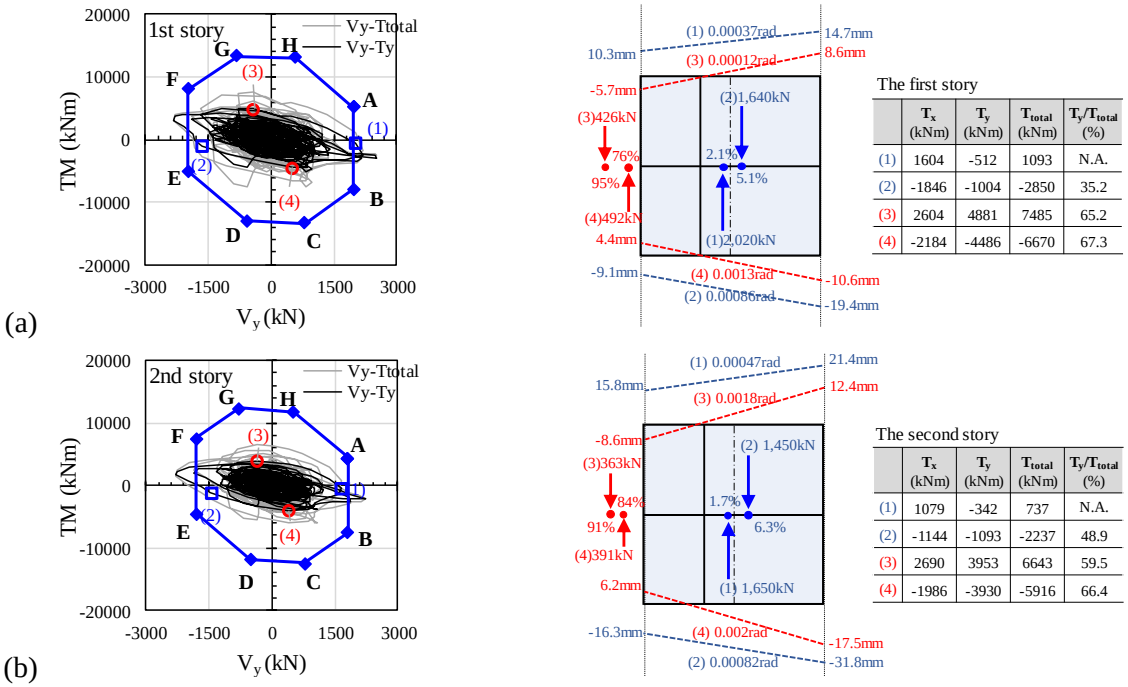

The first story

	T_x (kNm)	T_y (kNm)	T_{total} (kNm)	T_y/T_{total} (%)
(1)	1604	-512	1093	N.A.
(2)	-1846	-1004	-2850	35.2
(3)	2604	4881	7485	65.2
(4)	-2184	-4486	-6670	67.3

The second story

	T_x (kNm)	T_y (kNm)	T_{total} (kNm)	T_y/T_{total} (%)
(1)	1079	-342	737	N.A.
(2)	-1144	-1093	-2237	48.9
(3)	2690	3953	6643	59.5
(4)	-1986	-3930	-5916	66.4

(a)

(b)

Fig. 16 SST yield surface versus V_y-T response histories under DE in San Francisco: (a) 1st story; and (b) 2nd story

5. Conclusions

A new methodology in the seismic design and control of torsionally unbalanced building structures is presented in this paper. The followings are main features of this paper:

(1) Earthquake simulation tests on a 1:5 scale five-story RC building model with the irregularity of a soft/weak story and torsion at the ground story revealed that the eccentricity was not within the range specified by the code design eccentricity, but varied from zero to infinity and that even very small eccentricity can lead to the significantly large drift at the edge frame under the severe earthquake.

(2) To overcome the inappropriateness of the eccentricity as design parameter for torsion, a new methodology in the torsion design of torsionally unbalanced building structure is proposed by defining the design torsional moment in a direct relationship with the shear force given as an ellipse with the maximum points in its principal axes located by the two adjacent torsion-dominant modal spectral values. This approach provides a simple and transparent conceptual design tool through comparison with the torsion capacity diagram given as SST yield surfaces without having to perform dynamic time history analyses.

(3) The proposed approach to deal with the torsion behavior is demonstrated by taking a numerical example of a torsionally unbalanced five-story two-by-two bay RC building structure. In the design phase, the elliptical design demand obtained from the design spectrum and modal analysis appears to be within the SST yield surface (capacity). In the results of the nonlinear time history analyses of the structure, the SST yield surface represents well the strength distribution of each frame in torsion. Unlike the test results of the 1:5-scale model, in the analytical results the ratio of T_y/T_{total} are generally 55~70% regardless of the intensity of the input ground motion and despite the torsional stiffness degradation except for some instants when the peak translational behaviors in the Y direction are reached. At these peak translational drifts, most of the inertial torque is resisted by the perpendicular (X-dir.) frames or the X-directional and Y-directional frames torsionally counteract each other regardless of yielding of the Y-directional frames.

(4) The main concern in the torsion design is the control of the deformation and damage in the inelastic range rather than those in the elastic range. Therefore, further research for the proposed design approach is needed to control the inelastic behavior exceeding the SST yield surface.

Acknowledgments

The research presented herein was supported by the National Research Foundation of Korea (NRF-2007-0054740, NRF-2009-0078771, and NRF-2016R1C1B1016653) and the Korea University Grant (K1510481). The authors are grateful for these supports.

References

[1] Anagnostopoulos SA, Kyrkos MT, and Stathopoulos KG (2015): Earthquake induced torsion in buildings: critical review and state of the art. *Earthquakes & Structures*, **8**(2), 305-377.
[2] Lee HS, Jung DW, Lee KB, Kim HC, and Lee K (2011): Shake-table responses of a low-rise RC building model having irregularities at first story, *Structural Engineering & Mechanics*, **40**(4), 517-539.
[3] Lee HS, Lee KB, Hwang KR, and Cho CS (2013): Shake-table Responses of an RC Low-rise Building Model Strengthened with Buckling Restrained Braces at Ground Story. *Earthquakes & Structures*, **5**(6), 703-731.
[4] Lee HS and Hwang KR (2015): Torsion design implications from shake-table responses of an RC low-rise building model having irregularities at the ground story. *Earthquake Engineering & Structural Dynamics*, **44**, 907–927.
[5] Architectural Institute of Korea (AIK) (2005, 2009): Korean Building Code. *KBC 2005, 2009.* Seoul, Korea. (in Korean)
[6] De la Llera JC, and Chopra AK (1995): Understanding the inelastic seismic behavior of asymmetric-plan buildings. *Earthquake Engineering and Structural Dynamics*, **24**:549–572.
[7] Chopra AK and De la Llera JC (1996): Accidental and Natural Torsion in Earthquake Response and Design of Buildings. *Proceedings of 11th world conference on earthquake engineering*, Paper No. 2006, Acapulco, Mexico.
[8] Computers and Structures Inc. (2009): SAP 2000 [Software]. Computers and Structures, Inc.: Berkeley, CA.
[9] Computers and Structures Inc. (2013): ETABS 2013 [Software]. Computers and Structures, Inc.: Berkeley, CA.
[10] ASCE (2014): *Seismic evaluation and retrofit of existing buildings*. ASCE/SEI 41-13, Reston, VA.